

## Diurnal Cycle of Convective Activity and Environmental Conditions during the Heavy Rainfall Event of 4-9 July 2020 in the Yangtze-Huai River Valley Region

○Ling TONG, Tetsuya TAKEMI

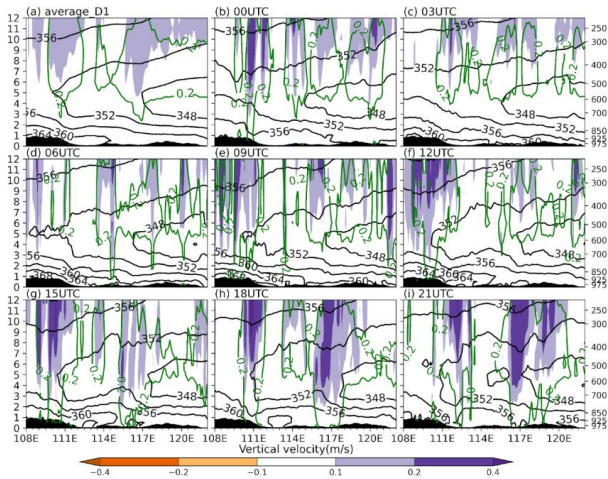
The characteristics of the diurnal cycle of convective activity and the environmental conditions for generating heavy rainfall over the Yangtze-Huai River Valley (YHRY) region are explored by using satellite data (CMORPH) and WRF simulations. An extreme case that occurred during 4-9 July 2020 was chosen in this study.

The observation indicated that regions of heavy rains fluctuate in meridional direction on a time scale from a few hours to days. The WRF simulation well captures this spatial and temporal patterns of the heavy rainfalls. Remarkable preferred regions of large amounts of rainfall were evident over the lower YHRV, with particular nocturnal rainfall enhancements within the active period, accompanied by obvious characteristics of eastward and southward movements. The simulation results also confirm that the model can grasp the characteristics of the observed precipitation activities. The total water condensate shows similar tendencies as the propagating features of the updraft and downdraft, which are favorable for the development of locally generated convective activities. The diurnal cycle of rainfall starts at night, reaches its maximum value in the early morning, and ends in the middle morning over the lower reach of the YHRV. Another peak occurs in the late afternoon between the middle and lower reaches of the YHRV. The maxima are reflected at 29°N–30°N in the nighttime and 28°N–29°N in the afternoon in the nearby vicinity of mountainous areas centered near 108°E–111°E, 112°E–114°E, and 116°E–118°E.

The analysis period is separated into 3 days from 5 to 7 July as the active period and 2 days from 8 to 9 July as the inactive period to compare the environmental features for the generation of the diurnal cycle of convection and rainfall.

During the active period, the locations and times of the convective activities and rainfall can be influenced by surface solar heating starting in the morning, which results in enhanced instability in the lower troposphere and in higher convective available potential energy (CAPE) values in the afternoon, especially in the mountainous areas, and thus leads to the development of deep moist convective activities. The nocturnal maximum results from the diurnal variation of local circulation forced by the complex terrain, especially the mountains, in combination with the steady enhancement of humidity at heights less than 6 km, stronger upward movements over the lower reach of the YHRV, and low-level winds favorable for inducing horizontal convergence. These environmental conditions favor the generation of convection and rainfall.

However, during the inactive period, the diurnal cycle of rainfall begins to show scattered distributions. The decrease of humidity cooperates with the convective inhibition (CIN) value in the lower troposphere and the expansion of the lower equivalent potential temperature, causing the middle-to-upper layer to die off. In the meantime, the ingestion of dry air further leads to suppression of the convective activities and to ending of the extreme rainfall.



projected in the cross section (the unit vector denoted at the upper right, in  $\text{m s}^{-1}$ ). (e) (f) CIN (color shading, in  $\text{J kg}^{-1}$ ) and the equivalent potential temperature (contours, in K). The black shading denotes topography.

Fig. 1 The composited vertical and zonal cross section (averaged for the  $28^{\circ}\text{N}$ – $31^{\circ}\text{N}$  band) of equivalent potential temperature (black solid line, in K), vertical velocity (color shading, in  $\text{m s}^{-1}$ ), total water condensate water mixing ratio ( $0.2 \text{ g kg}^{-1}$  contour, green solid line) for (a) the temporal averages from 5 to 7 July 2020 and for the spatial averages at (b) 00UTC, (c) 03UTC, (d) 06UTC, (e) 09UTC, (f) 12UTC, (g) 15UTC, (h) 18UTC, and (i) 21UTC. The results from D01 are indicated here. The black shading denotes topography.

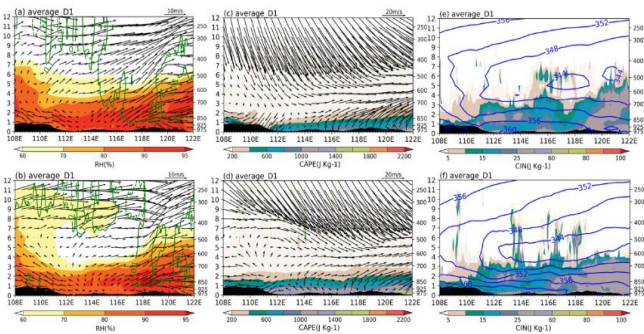


Fig. 2 The vertical and zonal cross section (averaged in the  $28^{\circ}\text{N}$ – $31^{\circ}\text{N}$  band) of the daily-mean fields averaged on 8 July 2020 ((a), (c), and (e)) and averaged on 9 July 2020 (b), (d), and (f)). (a) (b) Relative humidity (color shading, in %) and the zonal and vertical wind vector projected on the cross section (the unit vector denoted at the upper right, in  $\text{m s}^{-1}$ ), and convective momentum transport (green contour lines at  $-0.1$  and  $0.1 \text{ m}^2 \text{ s}^{-2}$ ). (c) (d) CAPE (color shading, in  $\text{J kg}^{-1}$ ) and the horizontal wind vector